N73-24662

NASA TM X-2797

# NASA TECHNICAL MEMORANDUM

NASA TM X-2797



# CAVITY TEMPERATURE AND FLOW CHARACTERISTICS IN A GAS-CORE TEST REACTOR

*by Henry A. Putre*

*Lewis Research Center*

*Cleveland, Ohio 44135*

NATIONAL AERONAUTICS AND SPACE ADMINISTRATION • WASHINGTON, D. C. • JUNE 1973

| 1. Report No. | 2. Government Accession No. | 3. Recipient's Catalog No. |
|---|---|---|
| NASA TM X-2797 | | |

| 4. Title and Subtitle | 5. Report Date |
|---|---|
| CAVITY TEMPERATURE AND FLOW CHARACTERISTICS IN A GAS-CORE TEST REACTOR | June 1973 |
| | 6. Performing Organization Code |
| 7. Author(s) | 8. Performing Organization Report No. |
| Henry A. Putre | E-7331 |
| | 10. Work Unit No. |
| 9. Performing Organization Name and Address | 503-04 |
| Lewis Research Center<br>National Aeronautics and Space Administration<br>Cleveland, Ohio 44135 | 11. Contract or Grant No. |
| | 13. Type of Report and Period Covered |
| 12. Sponsoring Agency Name and Address | Technical Memorandum |
| National Aeronautics and Space Administration<br>Washington, D. C. 20546 | 14. Sponsoring Agency Code |

15. Supplementary Notes

16. Abstract


A test reactor concept for conducting basic studies on a fissioning uranium plasma and for testing various gas-core reactor concepts is analyzed. The test reactor consists of a conventional fuel-element region surrounding a 61-cm- (2-ft-) diameter cavity region which contains the plasma experiment. The fuel elements provide the neutron flux for the cavity region. The design opering conditions include 60-MW reactor power, 2.7-MW cavity power, 200-atm cavity pressure, and an average uranium plasma temperature of 15 000 K. The analytical results are given for cavity radiant heat transfer, hydrogen transpiration cooling, and uranium wire or powder injection.


| 17. Key Words (Suggested by Author(s)) | | 18. Distribution Statement |
|---|---|---|
| Gas-core reactor | Test reactor | Unclassified - unlimited |
| Nuclear fuel | Radiant heat transfer | |
| Uranium plasma | | |

| 19. Security Classif. (of this report) | 20. Security Classif. (of this page) | 21. No. of Pages | 22. Price* |
|---|---|---|---|
| Unclassified | Unclassified | 25 | $3.00 |

* For sale by the National Technical Information Service, Springfield, Virginia 22151

# CAVITY TEMPERATURE AND FLOW CHARACTERISTICS IN A GAS-CORE TEST REACTOR

by Henry A. Putre
Lewis Research Center

## SUMMARY

A test reactor has been proposed for conducting basic studies on fissioning uranium plasmas and for testing various gas-core reactor concepts. The test reactor consists of a conventional driver fuel-element region surrounding a cavity region which contains a fissioning uranium plasma experiment. The driver reactor supplies the neutron flux for the cavity region. In the gas-core rocket simulation, uranium fuel is injected into the center of the cavity in solid form and is vaporized by fission heating. Seeded hydrogen "propellant" is injected through the cavity wall to protect the wall from the fuel-region radiant heat flux.

A radiant heat transfer analysis is used to calculate the cavity power and the transpiration propellant flow rate necessary to obtain high fuel-edge vaporization temperatures and low wall temperatures. For the design configuration of a 61-centimeter-(2-ft-) diameter cavity at a pressure of 200 atmospheres, the analysis predicts that these temperature conditions may be satisfied at a design cavity power of 2.7 megawatts, a hydrogen "propellant" flow rate of 0.046 kilogram per second, and a seed mass fraction of 0.25. However, at the resulting fuel-edge temperature of 6350 K, fuel vaporization may be marginal because of the uncertainty in fuel vapor pressure. By increasing the seed mass fraction to 0.35, the fuel-edge temperature is increased to 7000 K, and fuel vaporization is more probable.

A fuel-injection analysis is used to determine fuel feed system conditions required to prevent fuel melting inside the feeder tube and also to assure fuel vaporization near the cavity center. It was found necessary to use a neutron-absorbing feeder tube with a flux attenuation factor of 100. The desired fuel temperatures could be obtained with either 200-micrometer- (0.008-in.-) diameter uranium wire or 400-micrometer- (0.016-in.-) diameter powder. These sizes are probably within the operating range of mechanical feeders.

The propellant wall injection pressure drop tends to be very low. It is estimated that for controllable pressure drops of the order of 6900 newtons per square meter (1 psi) with 10 propellant injection slots, slot widths of 75 micrometers (0.003 in.) are required in the cavity wall. These may require intricate fabrication. Even if they can be fabricated, such small openings could be plugged by seed particles during operation. One way to circumvent this problem, should it become necessary to do so, would be to increase the propellant flow rate above the value required to thermally protect the cavity wall.

# INTRODUCTION

A conceptual design study has been carried out at the NASA Lewis Research Center of a gas-core test reactor for conducting experiments on a small fissioning uranium plasma held within a nuclear reactor cavity. This test reactor operates on the principle that gas-core-like conditions can be achieved in a small, subcritical, vaporized-fuel cavity region by locating most of the critical fuel mass in a separate, solid-fuel driver region. This principle was originally proposed as a mini-cavity gas-core rocket concept by Hyland (ref. 1). The main advantage of the mini-cavity concept was found to be that gas-core specific impulses (of 1500 sec or more) could be obtained in a smaller cavity size and with much lower power levels than those of the pure gas-core engine. In fact, the cavity size could be chosen independent of criticality requirements.

In the gas-core test reactor shown in figure 1(a), the separate driven reactor is used to supply a controlled neutron flux environment in a 61-centimeter- (2-ft-) diameter cavity region for testing various gas-core reactor concepts. A typical test cavity, shown schematically in figure 1(b), would have most of the major features of a full-scale gas-core rocket engine, except for absolute size and power. The cavity fuel is injected either as solid uranium or gaseous uranium hexafluoride ($UF_6$) and is fission heated. The fuel is vaporized in a central region, as shown in figure 1(b). Hydrogen "propellant," including some depleted uranium seed particles for radiant absorption, is injected through the cavity walls in a manner that causes least fuel entrainment and loss rate from the cavity. The propellant is heated primarily by thermal radiation from the fuel region. As in a gas-core engine, the heating and flow mechanisms in the test cavity determine the temperature conditions and the power and flow-rate requirements.

The purpose of this report is to summarize the analytical methods and results that were used to select the design conditions of the test reactor cavity for the conceptual design study. This report presents analytical estimates of the temperature and flow conditions that would exist in the test cavity. The specific questions that are addressed are:

(1) For a 61-centimeter- (2-ft-) diameter cavity and a reactor pressure of 200 atmospheres, what cavity power and propellant flow rate are required to obtain fuel edge vaporization and high propellant outlet temperatures without exceeding cavity wall temperature limits?

(2) What kind of fuel feed system is needed to get the uranium fuel (wire or powder) from the storage location outside the reactor through the moderator and into the cavity so that it vaporizes near the cavity center without plating out on the feed-tube walls?

(3) What are the requirements for the propellant injection flow passages for good fuel containment and propellant flow control?

# ANALYSIS

## Radiant Heat Transfer Analysis

The fuel- and propellant-region temperatures in the cavity are calculated with the use of a radiant heat transfer analysis with transpiration wall cooling as described by Kascak (ref. 2). The cavity model for this analysis and a typical temperature profile are shown in figure 1(c). The analysis assumes combined conduction, radiation, and convection heat fluxes in a one-dimensional, spherical geometry. The cavity is divided into a propellant and a fuel region. The propellant region has a specified radial propellant velocity profile with inflow at the wall and zero radial velocity at the fuel edge, and no heat sources. The fuel region has a local fission heating source strength that is proportional to the uranium fuel density and is assumed to have no convective heat transfer.

The energy-balance equations in terms of heat fluxes in the propellant region and in the fuel region, respectively, are

$$q_R + q_K - \frac{1}{r^2} \int_{R_W}^{r} \rho V r^2 \left(\frac{dh}{dr}\right) dr = \rho_W V_W (h_W - h_O) \left(\frac{R_W}{r}\right)^2 \qquad R_E < r < R_W \tag{1}$$

$$q_R + q_K = \frac{1}{r^2} \int_0^r S r^2 \, dr \qquad 0 < r < R_E \tag{2}$$

(Symbols are defined in the appendix.) The radiant heat flux is expressed in terms of the local temperature gradient by using the diffusion approximation,

$$q_R = -\frac{16}{3a_R} T^3 \frac{dT}{dr} \tag{3}$$

where the radiant absorption coefficient $a_R$ depends on temperature. The conduction heat flux includes both molecular and turbulent eddy transport.

Equations (1) and (2) are integrated numerically with the use of a computer code that includes temperature- and pressure-dependent properties of the hydrogen propellant, the seed material, and the uranium fuel. The specified parameters for the code are the cavity radius $R_C$, the fuel-edge radius $R_E$, the cavity pressure P, the uranium fuel partial pressure $P_u$, the hydrogen propellant flow rate $m_H$, the seed mass fraction X, and the propellant inlet temperatures $T_O$ and $T_W$. A radial flow profile V(r) is also specified. This analysis was used to obtain the plots of wall temperature as a function of cavity power for two propellant flow rates in figure 2. The required propellant flow for wall protection at various cavity powers is plotted for three different assumed flow profiles in figure 3.

The parametric variations of fuel-edge temperature and burnout power with pressure, propellant seed mass fraction, and propellant flow rate are plotted in figure 4. The temperature profiles in the cavity at both the wall-limit flow rate and the design flow rate are shown in figure 5. The matching plot for determining the driver reactor power and the cavity fuel mass is shown in figure 6.

## Fuel-Injection Analysis

This section presents the analysis of fuel-injection (uranium powder or wire) temperatures at axial locations in the feed tube and in the entry region of the cavity. A schematic of the feed-tube entry region is shown in figure 7. The fuel is heated by fissions during its travel through the feed tube into the cavity. The analysis applies to the initial cavity startup period, with full driver reactor power, cold cavity region, and no fuel in the cavity. The energy balance includes the fuel enthalpy change, the nuclear heating, and radiation losses to the cold surroundings. Convective cooling by the surroundings is neglected. The fuel enthalpy change along the cavity axis is

$$\frac{dh}{dt} = V_F \frac{dh}{dx} = \alpha - \frac{6\sigma\epsilon T^4}{\rho D} \tag{4}$$

where

$$V_F = \begin{cases} V_i + g(t - t_m) & \text{for wire} \\ V_t & \text{for powder} \end{cases} \tag{5}$$

These equations are solved for the axial distance where various state points (i.e., liquefaction at 1405 K, or vaporization at approximately 6500 K) occur. In general, the fuel velocity $V_F$ will depend on T and x, and the fission heating rate will have a value of $\alpha_T$ or $\alpha_C$, depending on whether the location is in the shielded feed tube or in the cavity. A uranium enthalpy-temperature relation, including heats of fusion and vaporization, is used. The uranium feed rate is specified, and the value of $\alpha_T = 0.01\ \alpha_C$ was assumed on the basis of a practical flux shielding factor in the feed tube.

Two distinct cases were thus treated. For wire fuel, the velocity up to the point of melting, $V_i$, is determined by the wire feed rate, and from melting, it is determined by gravity. The resulting fuel-wire temperature variation along the axis is shown in figure 8. For powder fuel, it was determined that the appropriate velocity is the settling, or terminal, velocity in hydrogen. (The hydrogen carrier-gas velocity is probably negligible compared to the terminal velocity.) The powder terminal velocity is determined by standard methods for spheres and is found to depend mainly on the particle diameter, as shown in figure 9(a). This velocity is assumed to be the same for a solid or liquid fuel particle. The temperature variation along the axis for powder fuel is shown in figure 9(b).

## DISCUSSION

The results of various cavity analyses are discussed in this section, in the following order:

(1) Cavity power and temperature conditions
(2) Cavity fuel mass and fuel vaporization conditions
(3) Fuel injection conditions
(4) Propellant injection requirements

### Cavity Power and Temperature Conditions

The cavity heat-transfer analysis requires input data for the fuel concentration and the fuel-region size to determine the fission heat-source distribution. These data depend on the fuel-containment characteristics of the cavity flow, which have been studied mostly in cold-flow simulation experiments. The best experimental results to date (ref. 3) indicate that at the cavity design values of propellant-to-fuel flow ratio of 40 and fuel-to-propellant density ratio of about 7.0, the effective fuel-volume fraction would be about 0.17 percent. This corresponds to a fuel region having a fuel partial-pressure ratio of 0.68 in a volume that occupies 25 percent of the cavity volume. Thus, for the cavity analysis, the assumed values are $R_F = (0.25)^{1/3} R_C = 0.192$ meter, and $P_u = 0.68 \times 200 = 136$ atmospheres.

For high cavity temperatures (to assure fuel vaporization and high specific impulse), it is desirable to operate the cavity near the wall transpiration cooling limit. The behavior of the wall temperature near this wall cooling limit is shown in figure 2. These results are for a cavity diameter of 61 centimeters (2 ft), a cavity pressure of 200 atmospheres, and a propellant inlet temperature of 300 K. The seed mass fraction $X$ is 0.25, and the seed radiant absorption coefficient is 25 000 square centimeters per gram.

For the design cavity power of 2.7 megawatts and an assumed cavity inner wall temperature of 600 K, the minimum wall-cooling flow rate is 0.038 kilogram per second. That is, at this flow rate, the inside wall temperature is well within wall material limits. However, figure 2 shows that at slightly higher powers (at 0.038-kg/sec flow rate), the wall temperature quickly increases to several thousand degrees. In order to provide an extra cooling margin in the event of cavity power surges, the design flow rate is chosen at 20 percent above the wall cooling limit, or 0.046 kilogram per second. This design flow rate maintains a safe wall temperature for up to 30 percent power surges (to 3.6 MW).

The sensitivity of the calculated wall cooling-limit flow rates to the assumed radial flow profile is shown in figure 3. The flow profile is an input to the analysis that has not been accurately determined. Various assumed profiles of radial mass flux are shown in figure 3(a). Profile 1 represents constant radial mass flux, which gives best wall protection, and profile 3 represents strong flow turning, with less wall protection. For the purpose of selecting a design propellant flow, a nominal profile with moderate flow turning (profile 2) has been used in figure 2. The effect of the flow profile on the limiting flow rate is shown in figure 3(b). At the design cavity power of 2.7 megawatts, the use of profile 2 yields a limiting flow rate of 0.038 kilogram per second (also see fig. 2). This value may vary from 0.026 kilogram per second for profile 1 to 0.047 kilogram per second for profile 3. In comparison, the design flow rate of 0.046 kilogram per second accommodates most of the possible uncertainty in the flow profile. For the purpose of this preliminary study, the design flow rate of 0.046 kilogram per second is based on calculations with profile 2. This appears adequate. This same profile is also assumed in all of the results that follow. Figure 4 shows the variation of fuel-edge temperature and cavity power at the wall cooling limit with various cavity parameters. The cavity pressure, propellant seed mass fraction, and propellant flow rate are varied in figures 4(a) to (c), respectively, about the design values of $P = 200$ atmospheres, $X = 0.25$, and $Q = 2.7$ megawatts. The fuel-edge temperature for the design case is 6350 K.

The pressure dependence displayed in figure 4(a) shows that both the cavity power and the fuel-edge temperature increase directly with pressure. For pressures ranging from 100 to 300 atmospheres, the cavity power increases from 2.0 to 3.3 megawatts, and the fuel-edge temperature increases from 5250 to 7150 K.

The effect of propellant seed mass fraction $X$ is shown in figure 4(b). The cavity power first increases with $X$, goes through a maximum at approximately $X = 0.25$, then decreases slowly with $X$. This is probably because, at small increasing values of $X$, the propellant radiant absorption coefficient is increased and the wall protection is increased. However, larger amounts of seed tend to reduce the heat capacity of the propellant. This reduces the wall protection at large $X$ values. For seed mass fraction increasing from 0.25 to 0.5, the power stays near 2.7 megawatts, whereas the fuel-edge temperature increases from 6350 to 7700 K.

For increasing propellant flow rate, as shown in figure 4(c), the cavity power increases approximately with the 1.5 power of flow rate. For propellant flow rate increasing from 0.038 to 0.05 kilogram per second, the power increases from 2.7 to 4.2 megawatts, and the fuel-edge temperature increases from 6350 to 6900 K.

As will be discussed in the next section, an increase in fuel-edge temperature may be desirable to assure complete fuel vaporization. The results of figure 4 indicate that an increase in fuel-edge temperature from 6350 to 7700 K can be obtained by increasing the propellant seed mass fraction from 0.25 to 0.50. This allows other conditions such as cavity power, pressure, and propellant flow rates to be essentially unchanged.

A complete set of design conditions has been selected on the basis of these results. This set is given in table I. The temperature profiles for the cavity are shown in figure 5. The solid curve is for the design conditions and the design propellant flow rate of 0.046 kilogram per second. For comparison, the dashed curve is for the wall cooling limit flow of 0.038 kilogram per second. It is seen that the propellant flow rate affects mainly the propellant-region temperatures near the wall. At the design flow rate (20 percent above the wall cooling limit), the propellant transpiration cooling forces the temperature edge away from the wall, thus assuring wall protection.

At the design flow and design power, the propellant outlet temperature is 3500 K. This corresponds to an ideal specific impulse of 1134 seconds and an exhaust "thrust" of 507 newtons (114 lbf).

## Cavity Fuel Mass and Fuel Vaporization Conditions

The cavity fuel mass is determined by integrating the radial distribution of the uranium density obtained from the calculated temperature profiles (see fig. 5) and the assumed fuel partial-pressure ratio of 0.68. For the design power of 2.7 megawatts, the fuel mass is estimated to be 572 grams. Because of the neutron flux coupling, the cavity power is related to the driver reactor power through the fuel mass. In fact, as is shown in figure 6, the cavity thermodynamics give one curve of cavity power as a function of fuel mass, whereas, neutronics give a second set of curves at various driver powers. The constant driver power curves are based on neutron flux profiles for a typical driver reactor configuration (light water moderator, beryllium reflector, and MTR-type fuel elements). The intersections of these curves, where the fuel mass is matched, are used to determine the design values of driver and cavity power. Figure 6 shows that at a cavity power of 2.7 megawatts, the cavity contains 572 grams of fuel, which in turn requires a driver power of 60 megawatts.

The fluid mechanics phenomena of the fuel containment in the actual cavity are probably more complicated than in the cold-flow simulation tests on which present estimates of fuel volume fraction are based. In fact, hot flows may have less mixing and better fuel containment than cold flows. This possibility should be studied in hot-flow tests. However, the cavity would also operate at a higher "buoyancy" condition, with downward flow (i.e., the tendency of the heavier fuel to sink through the propellant because of gravity), than in the cold-flow experiments. This downward flow has been observed in references 4 and 5 to have reduced fuel containment. The net effect could be to reduce the cavity fuel mass below that presently estimated. On the other hand, recent experiments with upward flow indicate that it may be possible to reduce or even use to advantage the buoyancy effect and thus to increase the fuel mass by designing the cavity so that it exhausts upward. In the event that the fuel containment is less than was estimated, the major effect on the cavity conditions is to shift the thermodynamics curve in figure 6 to the left. Thus, the cavity power could still be maintained at the design value, but at the expense of increased driver power.

In order to assure fuel vaporization, the fuel-edge temperature should exceed the vaporization temperature at the fuel-region partial pressure (136 atm). The relation between vapor pressure and temperature at high temperatures for uranium is not accurately known. From an equation given in reference 6, which fits uranium data up to 2200 K, the fuel vaporization temperature at 136 atmospheres is estimated to be 6700 K. This is above the calculated fuel-edge temperature of 6350 K. The difference here is probably within the range of uncertainty in the vapor-pressure extrapolation. Thus, fuel vaporization in about a 1-millimeter-thick region at the fuel edge may be marginal, and the cavity conditions may need to be adjusted to raise the fuel-edge temperature by some nominal value, say 500 K. Figure 4 indicates that a simple way to accomplish this, without changing the cavity power or pressure, is to increase the propellant seed mass fraction from 0.25 to about 0.35. This allows all other conditions to be unchanged and results in a fuel-edge temperature of 7000 K. However, the capability of feeding hydrogen with a larger seed mass fraction needs further experimental investigation.

## Fuel Injection Conditions

The uranium cavity fuel is supplied to the cavity through a feed tube as shown in figure 7. The main requirements for the fuel injection system are that the fuel must pass through the feed tube without melting or depositing on the inner surface of the feed tube, and that the fuel vaporization point must be located within the designated vaporized-fuel region (i.e., $L_v$ in fig. 7 must be between 11.43 cm (4.5 in.) and 49.53 cm (19.5 in.)). Ideally, as shown in figure 7, the fuel would leave the feed tube as a solid and would liquefy at a distance $L_m$ from the inlet. The liquid would continue flowing downward because of gravity and would vaporize at a distance $L_V$ before dispersing as fuel vapor. These distances are determined from the calculated axial fuel temperature profiles in figures 8 and 9.

The fuel temperature profiles are different during cavity startup than during steady-state operation. During steady-state operation (with hot fuel-and-propellant surroundings), the injected-fuel temperatures in the cavity follow the propellant-region temperatures (see fig. 6) very closely because of strong radiant heating from the seeded propellant. Thus, by definition, vaporization of injected fuel, whether wire or powder, is assured inside the fuel vapor region. However, during the cavity startup (with cold surroudings and about three times the steady-state neutron flux, because there is no fuel in the cavity), the fuel loses heat by radiation and is less likely to vaporize at the proper location. The results of the analysis for the startup case are now discussed.

Equation (4) was solved for both wire and powder fuel to give the centerline fuel temperature variation in the feed tube (through the reflector) and in the cavity region. The energy balance includes the fuel heat capacity, the fission heating, and the radiation loss to cold surroundings. The radiation loss was included since at temperatures near vaporization (above about 5000 K) this term may approach the fission heating rate, and for small particle sizes, radiation loss may actually result in a maximum particle temperature that is below the vaporization temperature.

Preliminary calculations indicated that flux attenuation in the feed tube was desirable. As a reference case, a fuel heating rate of 15 kilowatts per gram was used. This corresponds to the unfueled cavity at the design driver power of 60 megawatts and, because of reduced flux attenuation, is about three times the heating rate for the filled, steady-state cavity. A flux attenuation factor of 100 was used for the feed tube. This factor can be achieved by wrapping the feed tube with 0.40 millimeter (0.016 in.) of cadmium or 0.90 millimeter (0.035 in.) of 3-percent-boron steel. Thus, a value of 15 kilowatts per gram was used for $\alpha_C$, and 0.15 kilowatt per gram was used for $\alpha_T$. The design uranium flow rate of 1.15 grams per second (0.0025 lb/sec) and a 30.5-centimeter- (1-ft-) thick reflector were used. The fuel surface emissivity $\epsilon$ was assumed to be 0.1, a reasonable but conservative value for hot metal.

The temperature variation for the wire fuel is shown in figure 8. The figure shows that for the range of wire diameters from 142 to 250 micrometers (0.0056 to 0.010 in.), the vaporization point falls within the desired fuel region. The feed-tube exit (cavity-inlet) temperature for three wire sizes is below 500 K, which is well below the uranium melting point of 1405 K. Thus, the feed temperature in the feed tube is probably well within tube material limits. The wire feed velocity ranges from 3.6 meters per second (12 ft/sec) for the 142-micrometer (0.0056-in.) wire to 1.2 meters per second (4 ft/sec) for the 250-micrometer (0.010-in.) wire. Because of their larger velocity for the same total feed rate, the smaller wires travel farther into the fuel vapor region before vaporizing. For wire sizes larger than about 250 micrometers (0.010 in.), the low velocity results in fuel vaporization upstream of the desired region. On the other hand, for wire sizes smaller than 142 micrometers (0.0056 in.), the radiation cooling delays vaporization until the wire is past the desired fuel vapor region, or it may prevent vaporization altogether. Note that the effect of gravity accelerating the wire after it melts and reducing the wire diameter has been included in figure 8.

The terminal velocity for the uranium powder is shown as a function of particle diameter in figure 9(a). The temperature variation for uranium powder feed is shown in figure 9(b). In contrast with the wire feed, the largest particles have the largest terminal velocity and travel farthest before vaporizing. The curvature of the temperature profiles in figure 8 is due to the radiant cooling.

The range of particle sizes for which the vaporization point falls inside the desired fuel region is shown in figure 8 to be 210 to 600 micrometers (0.0083 to 0.024 in.). The corresponding range of teminal velocity is about 2.7 to 6.1 meters per second (about 9 to 20 ft/sec). Particles smaller than 210 micrometers (0.0083 in.) may not vaporize in the fuel region because of radiant cooling. For particles greater than 600 micrometers (0.024 in.), the larger velocity results in fuel vaporization downstream of the desired region. As with the wire fuel, the feed tube exit temperature with powder fuel is below 500 K.

As stated in the Fuel-Injection Analysis section, these results neglect convective cooling, which will tend to adversely increase the powder or wire size at the radiation cooling limit. However, a more accurate determination of the cooling-limit size requires more accurate data of vapor pressure as a function of temperature for uranium than are now available.

The present approximate analysis has identified the particle size (or wire diameter), the fission heating rate per gram of fuel, and the fuel flow rate as the major parameters that determine the location where the injected fuel vaporizes. The desirable nominal fuel size is about 200-micrometer (0.008-in.) wire diameter or 400-micrometer (0.016 in.) particle diameter. Both of these are probably within the operating limits for mechanical feeders. The results also show that the feed-tube exit temperature is below 500 K for these sizes.

## Propellant Injection Requirements

The propellant-injection flow passages in the cavity wall must be designed to satisfy various requirements, including the following:

(1) The injection angle and the axial variation of flow should be tailored for best fuel containment.

(2) The flow passages should be relatively closely spaced to provide a uniform wall film for transpiration cooling and to provide uniform radiation protection.

(3) The flow passages (slots, holes, or pores) should be large enough for injecting hydrogen with seed particles without plugging.

(4) The pressure drop across the wall should be sufficient (probably of the order of 6900 $N/m^2$ (1 psi)) to permit reasonable flow control with a high pressure regulating system.

The combination of requirements (1) to (3) tends to set a lower limit on cavity-wall flow-passage area. The main problem being discussed here is that for an assumed minimum propellant injection area that satisfies requirements (1) to (3), at the design propellant flow rate of 0.046 kilogram per second, there may not be enough wall pressure drop to satisfy requirement (4).

As an example, the wall pressure drop is calculated for a typical flow-passage configuration using slots (fig. 10(a)). Configurations using holes (fig. 10(b)) or porous walls (fig. 10(c)) may also be used. However, only the slotted wall is discussed herein. The typical slotted-wall arrangement in figure 10(a) is based on recent fuel-containment experiments (refs. 4 and 5) which have indicated that at least 10 axial injection stations with injection angles of approximately $15^{\circ}$ are required for reasonable fuel-containment characteristics. The slot width, which ranges from 0.25 to 0.64 centimeter (0.10 to 0.25 in.) in the experiments, will be considerably smaller in the test reactor cavity. A 0.64-centimeter- (0.25-in.-) thick cavity wall is assumed, and this gives a slot depth through the wall of 2.5 centimeters (1.0 in.). The slots are assumed to have a 50-percent open area.

For simplicity herein, pure hydrogen flow at 450 K and 200 atmospheres is assumed.

The calculated wall pressure drop (including inlet and exit losses plus friction pressure drop) is plotted for several propellant flow rates as a function of slot width in figure 11. It is seen that for a minimum slot width of 250 micrometers (0.010 in.), based on seeded flows, the pressure drop at the design flow is 210 newtons per square meter (0.03 psi). On the other hand, a wall pressure drop of 6900 newtons per square meter (1 psi) requires slots as small as 76 micrometers (0.003 in.). This size may be too small to fabricate or may be plugged by seed particles during operation.

As an alternative, increasing the propellant flow rate by a factor of five to 0.230 kilogram per second (0.5 lb/sec) as shown in figure 11, would allow use of 200-micrometer (0.008-in.) slots for a pressure drop of 6900 newtons per square meter (1 psi). However, the heat-transfer analysis indicates that at the design cavity power of 2.7 megawatts, this flow increase would decrease the fuel-edge temperature from 6350 to 5100 K, and fuel condensation would probably result. Also, the specific impulse would decrease from 1230 to 540 seconds.

These results indicate that it may be difficult to achieve a wall pressure drop of 6900 newtons per square meter (1 psi), should this be a requirement for propellant flow control. As an alternative, the possibility of controllable wall injection with 250-micrometer- (0.010-in.-) slots and a pressure drop of 210 newtons per square meter (0.03 psi) should be investigated further. Also, the possibility of using another propellant gas with different heat-transfer and pressure-drop characteristics should be investigated.

## SUMMARY OF RESULTS

The results of the cavity heat-transfer analysis indicate that for the 0.61-meter- (2-ft-) diameter cavity with a design cavity power of 2.7 megawatts, the minimum propellant flow rate required to maintain the wall temperature within the temperature limits of the material is 0.038 kilogram per second. This assumes a propellant seed mass fraction of 0.25 and a cavity pressure of 200 atmospheres. The design propellant flow rate of 0.046 kilogram per second is 20 percent above this wall cooling limit and provides additional wall protection. At these design conditions, the propellant outlet temperature is 4150 K, which corresponds to a specific impulse of 1134 seconds and a "thrust" of 114 pounds. The corresponding fuel-edge temperature is 6350 K.

At these conditions, the fuel is vaporized over the entire fuel region, except possibly for a 1-millimeter thick region near the fuel edge, where temperatures may be below vaporization. To assure fuel vaporization in this region, it may be desirable to increase the propellant seed mass fraction from the design value of 0.25 to 0.35.

The estimated cavity fuel mass is 572 grams. The driver reactor power (for a $H_2O$ moderated system) corresponding to this fuel mass and to the cavity power of 2.7 megawatts is 60 megawatts. The driver reactor should be designed for higher powers than this to maintain the cavity power in the event that the effective fuel volume fraction (or contained fuel mass) is lower than estimated.

The results of a fuel injection heating analysis indicate that the fuel feed tube should be clad with a neutron absorber (cadmium or borated stainless-steel sheet) capable of reducing the neutron flux by a factor of about 100. The desired fuel conditions (less than 500 K within the feed tube and vaporization near the cavity center) were found to be achievable by a narrow range of fuel wire and powder sizes. It was concluded that either a 200-micrometer- (0.008-in.-) diameter uranium wire or 400-micrometer- (0.016-in.-) diameter particles would be feasible. These sizes are probably suitable for mechanical feeder operation.

The propellant injection through the cavity wall, with controllable wall pressure drops of the order of 6900 newtons per square meter (1.0 psi), will require extremely small flow passages. Assuming 10 slot locations for good wall flow distribution, the required slot width is 76 micrometers (0.003 in.). This size may be difficult to fabricate, or may cause seed blockage. One way to circumvent this problem would be to increase the propellant flow rate considerably above the value required to thermally protect the cavity wall.

Lewis Research Center,
National Aeronautics and Space Administration,
Cleveland, Ohio, March 1, 1973,
503-04.

# APPENDIX - SYMBOLS

| | |
|---|---|
| $a_R$ | Rosseland mean radiant absorption coefficient |
| D | fuel powder diameter, or 1.5 times the fuel wire diameter |
| g | earth gravity constant |
| h | enthalpy |
| $L_m$ | length from feed-tube inlet to point where fuel melts |
| $L_v$ | length from feed-tube inlet to point where fuel vaporizes |
| $m_H$ | propellant flow rate |
| P | cavity pressure |
| $P_u$ | uranium fuel partial pressure in fuel region |
| Q | total cavity power |
| $q_K$ | conductive heat flux in cavity |
| $q_R$ | radiant heat flux in cavity |
| R | radius |
| r | radius distance |
| S | fuel fission heating per unit volume |
| T | temperature |
| t | time |
| $t_m$ | time to fuel melting |
| V | local radial propellant velocity |
| $V_i$ | initial fuel wire feed velocity |
| $V_t$ | fuel powder terminal velocity |
| X | uranium seed mass fraction in propellant |
| x | distance along fuel feed path from cavity inlet |
| $\alpha_T, \alpha_C$ | fuel fission heating in feed tube, or cavity |
| $\epsilon$ | fuel emissivity |
| $\sigma$ | Stefan-Boltzmann constant |
| $\rho$ | local density |

Subscripts:

| | |
|---|---|
| E | fuel edge |
| F | fuel |
| C | cavity |
| O | outer wall surface |
| W | inner wall surface |

# REFERENCES


1. Hyland, Robert E.: A Mini-Cavity Reactor for Low-Thrust High-Specific Impulse Propulsion. J. Spacecraft Rockets, vol. 9, no. 8, Aug. 1972, pp. 601-606.

2. Kascak, A. F.: Nozzle and Cavity Wall Cooling Limitations on Specific Impulse of a Gas-Core Nuclear Rocket. 2nd Symposium in Uranium Plasmas: Research and Applications. AIAA, 1971, pp. 173-178.

3. Bennett, John C.; and Johnson, Bruce V.: Experimental Study of One- and Two-Component Low-Turbulence Confined Coaxial Flows. NASA CR-1851, 1971.

4. Johnson, Bruce V.: Exploratory Study of the Effects of Injection Configurations and Inlet Flow Conditions on the Characteristics of Flow in Spherical Chambers. NASA CR-1965, 1972.

5. Kunze, J. F.; Suckling, D. H.; and Cooper, C. G.: Flowing Gas, Non-Nuclear Experiments on the Gas Core Reactor. Rep. ANCR-1032, Aerojet Nuclear Co. (NASA CR-120824), Feb. 1972.

6. Pattoret, A.; Smoes, S.; and Drowart, J.: Thermodynamic Studies of the Uranium-Oxygen System by Mass Spectrography. The Heat of Sublimation of Uranium. Euratom Rep. EUR-2458, 1965. (Trans. by Dunreay Experimental Reactor Establishment, Dunreay-224, 1966.)

TABLE I. - CAVITY DESIGN-POINT CONDITIONS

| | |
|---|---|
| Cavity diameter, m (ft) | 0.609 (2) |
| Cavity pressure, atm | 200 |
| Cavity power, MW | 2.7 |
| Propellant/fuel flow-rate ratio | 40 |
| Fuel/propellant density ratio | 7.5 |
| Cavity power at wall cooling limit, MW | 3.6 |
| Driver region power ($H_2O$ moderator), MW | 60 |
| Fuel region diameter, m | 0.384 |
| Fuel region uranium partial pressure, atm | 136 |
| Fuel-edge temperature, K | 6350 |
| Fuel centerline temperature, K | 20 300 |
| Average fuel temperature, K | 15 100 |
| Uranium fuel flow rate, kg/sec | 0.00115 |
| Uranium fuel mass in cavity, kg | 0.572 |
| Average fuel density, $kg/m^3$ | 19.2 |
| Hydrogen plus seed propellant flow rate, kg/sec | 0.046 |
| Propellant seed mass fraction | 0.25 |
| Propellant inlet temperature, K | 300 |
| Inside cavity-wall temperature, K | 600 |
| Average propellant-region temperature, K | 2550 |
| Propellant exit temperature, K | 4150 |
| Average propellant density, $kg/m^3$ | 2.56 |
| Ideal specific impulse, sec | 1134 |
| Ideal thrust, N (lb) | 507 (114) |

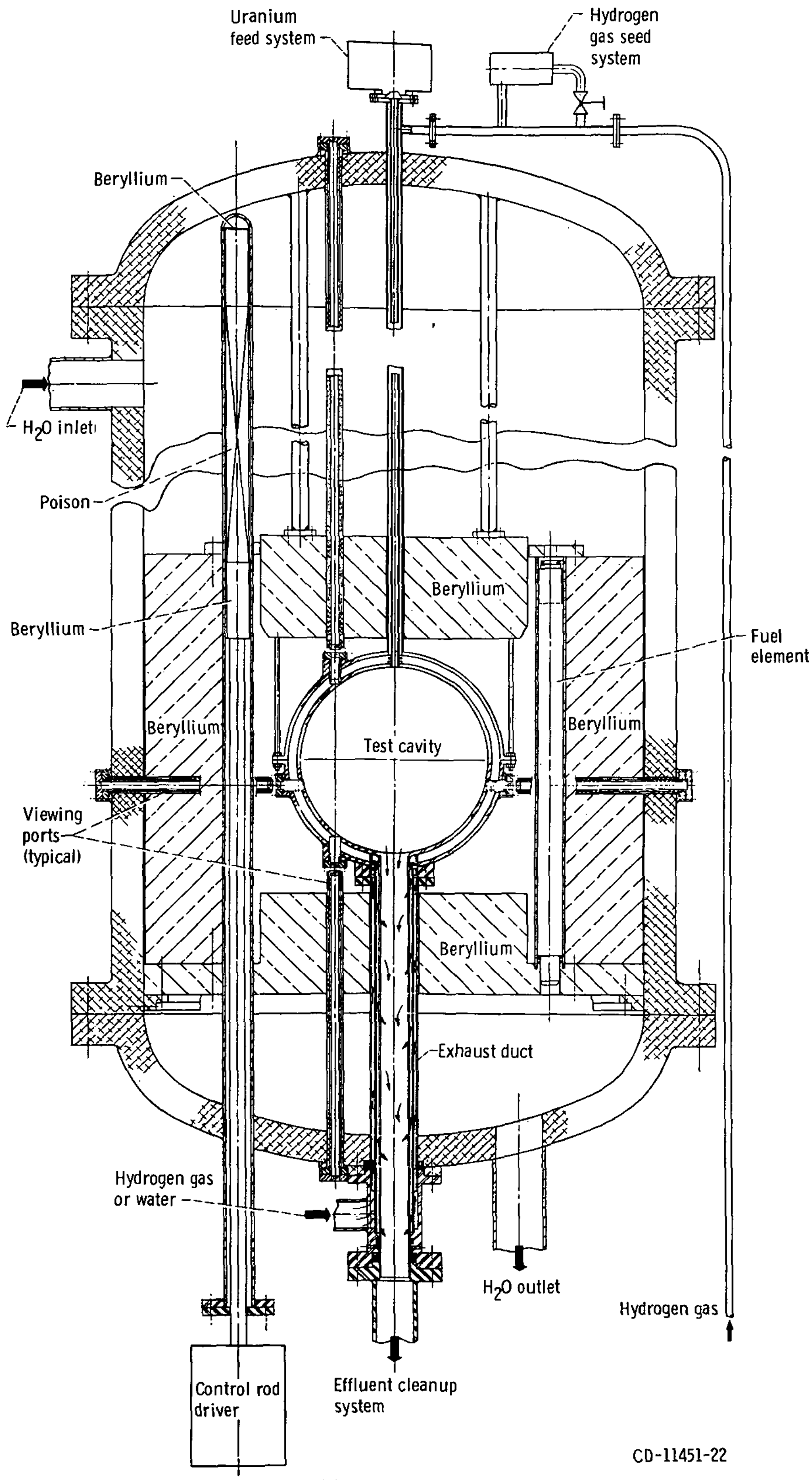


(a) Gas core test reactor.

Figure 1. - Schematic diagram and analysis model of test cavity.

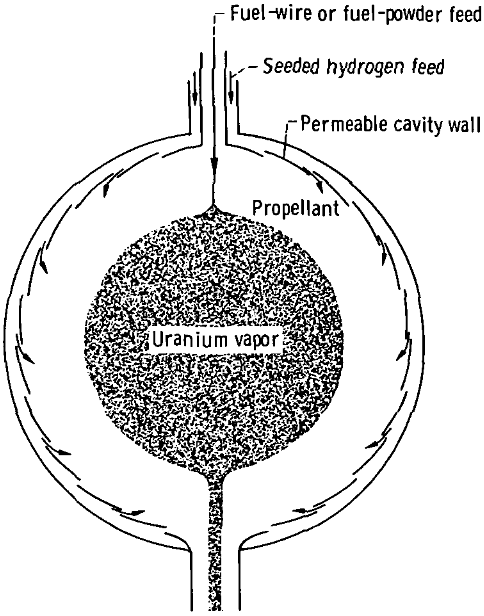


(b) Schematic of test cavity.

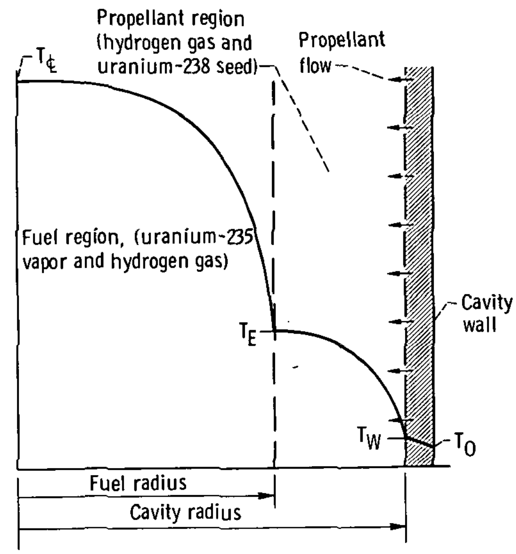


(c) Model for radiant heat transfer analysis, showing typical temperature profile.

Figure 1. - Concluded.

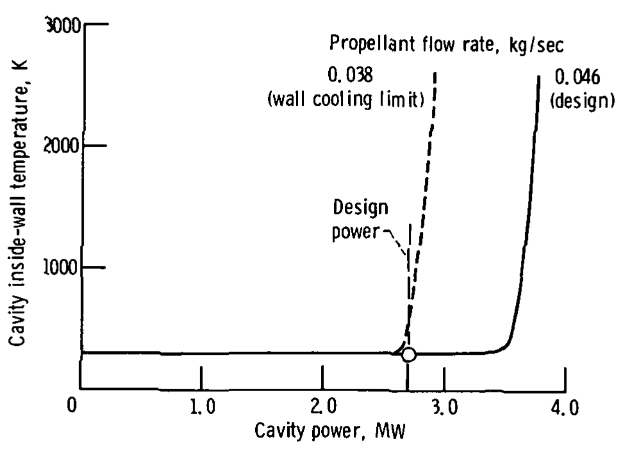


Figure 2. - Cavity wall temperature as function of cavity power for constant propellant flow rates. Outside wall temperature, 300 K.

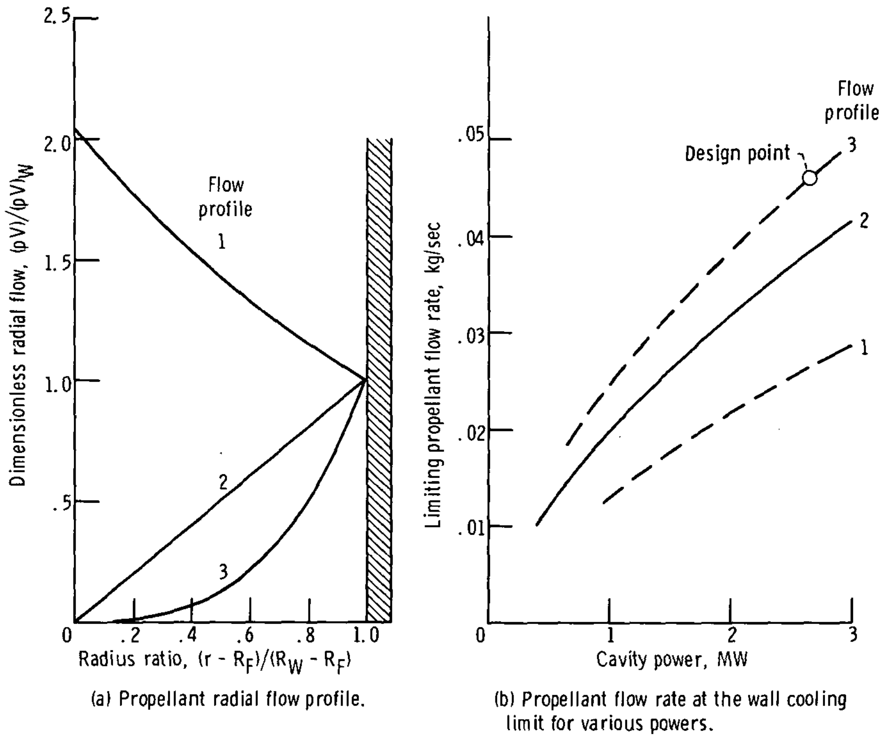


Figure 3. - Propellant radial flow profiles and limiting flow rate for various cavity powers.

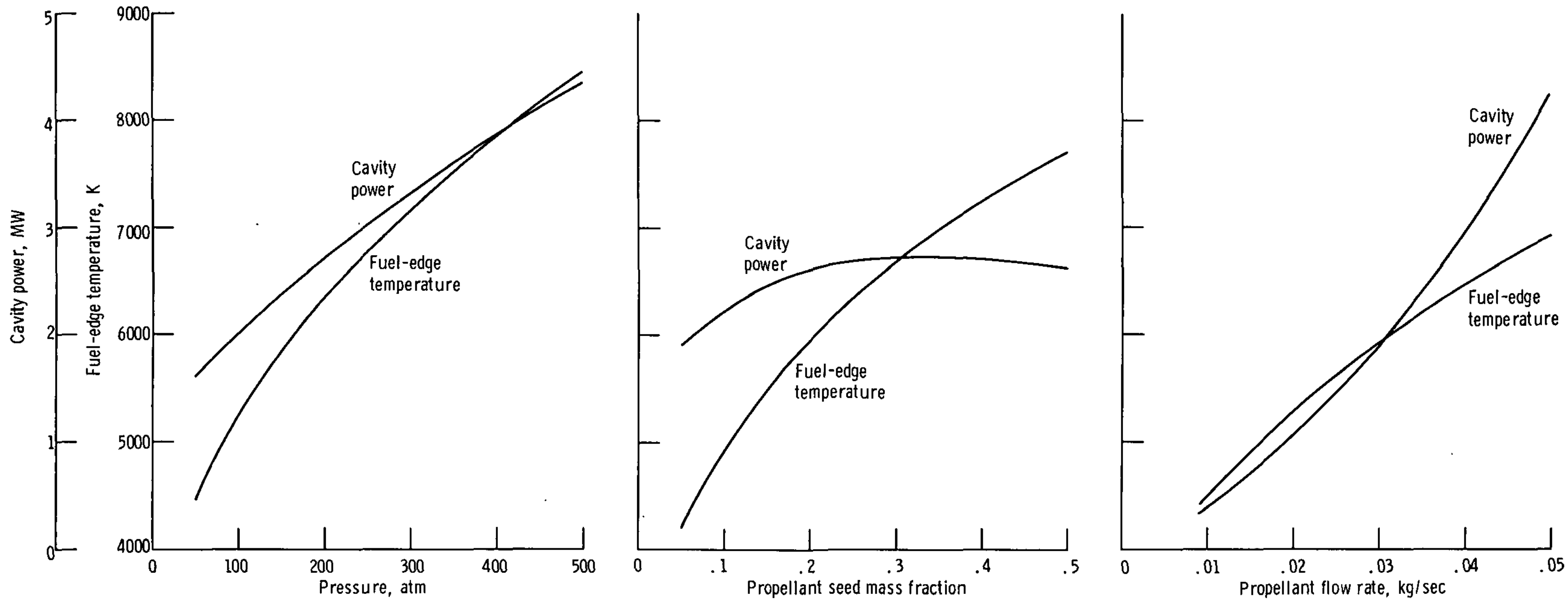


(a) Variation with pressure.

(b) Variation with propellant seed mass fraction.

(c) Variation with propellant flow rate at the wall cooling limit.

Figure 4. - Variation of fuel-edge temperature and cavity power with pressure, propellant seed mass fraction, and propellant flow rate.

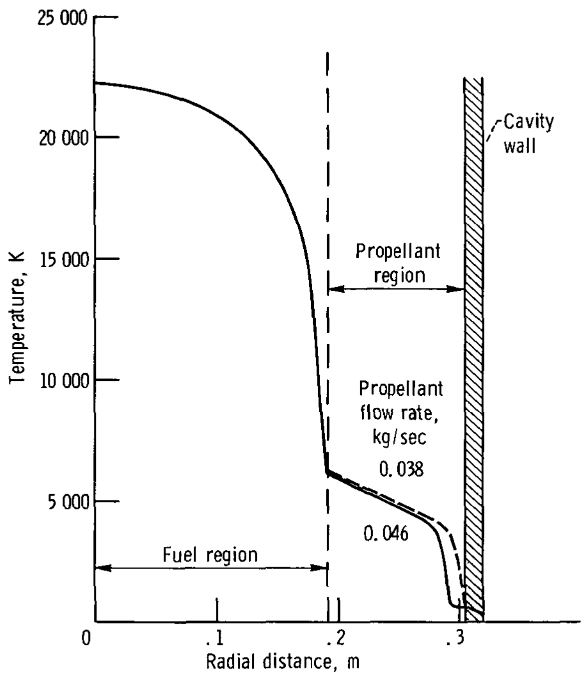


Figure 5. - Cavity temperature profiles at the wall cooling limit flow rate and the design flow rate. Total cavity power, 2.7 megawatts.

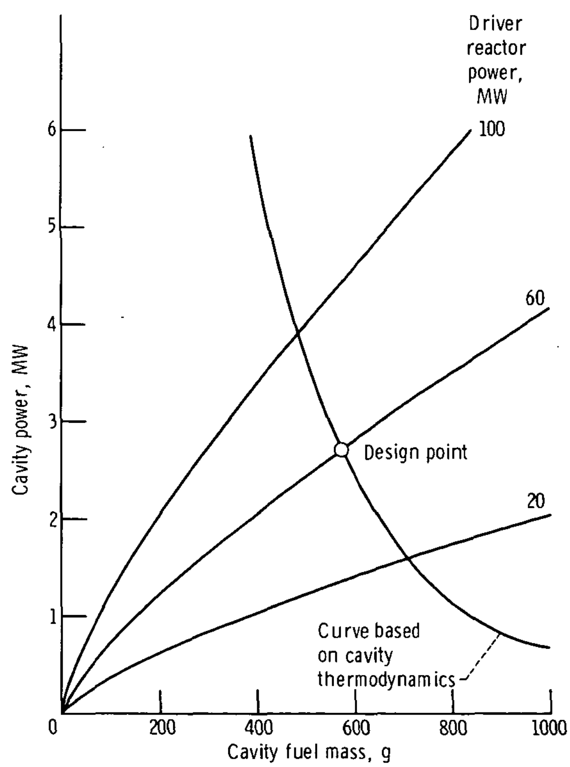


Figure 6. - Cavity power variation with cavity fuel mass for various driver powers.

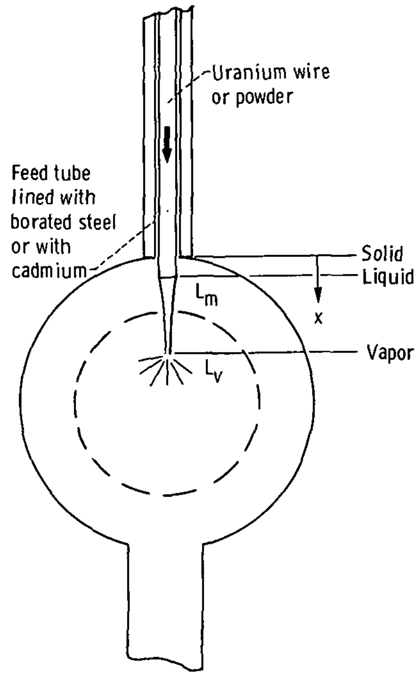


Figure 7. - Schematic of uranium fuel feed tube.

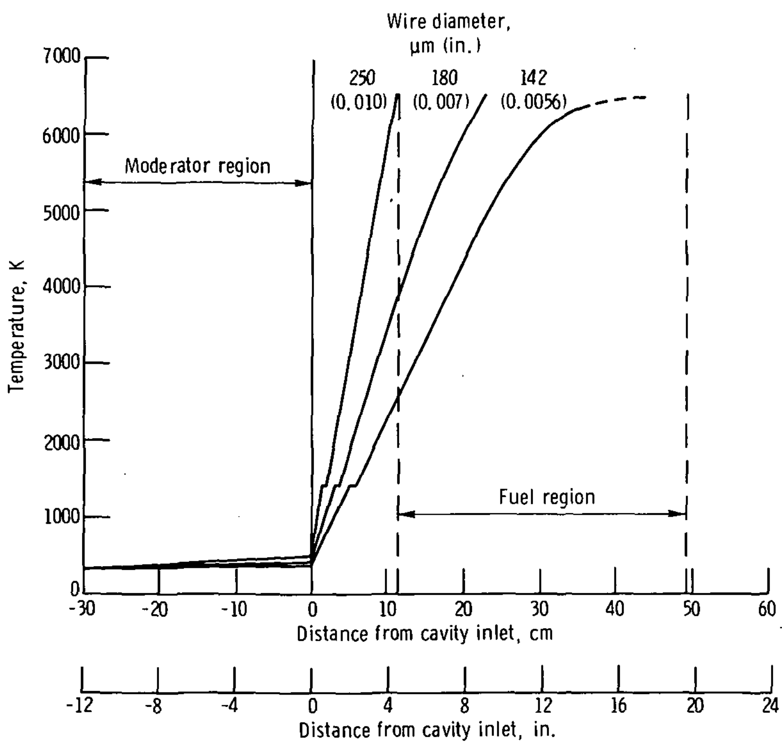


Figure 8. - Fuel-wire temperature variation along axis.

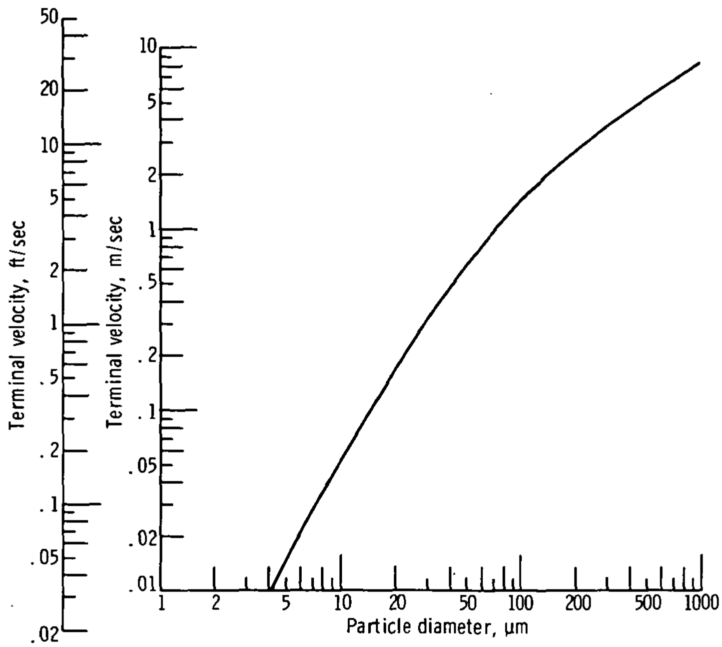


(a) Particle terminal velocity for various particle sizes (uranium particles in hydrogen).

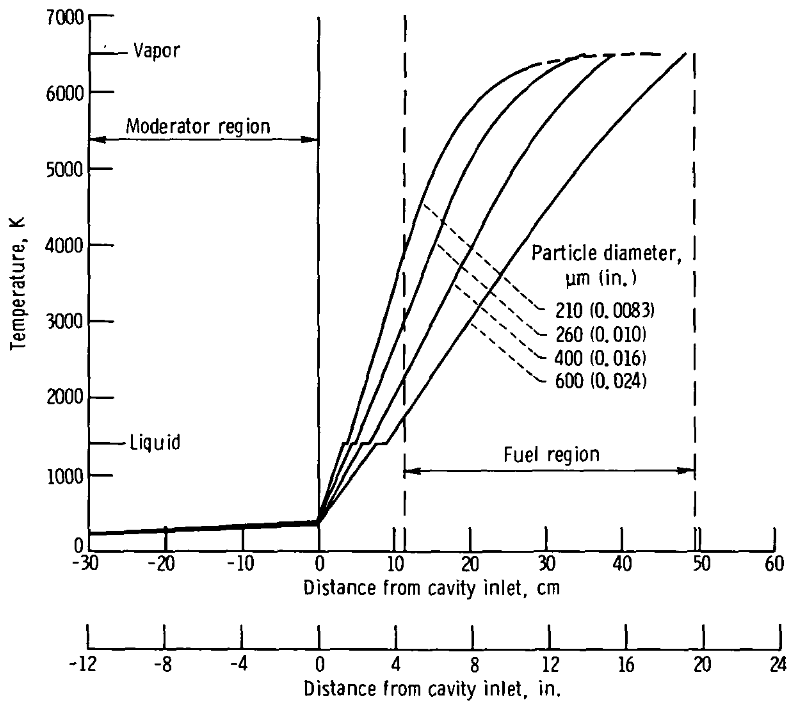


(b) Fuel-powder variation along axis.

Figure 9. - Terminal velocity and temperature variation for fuel powder.

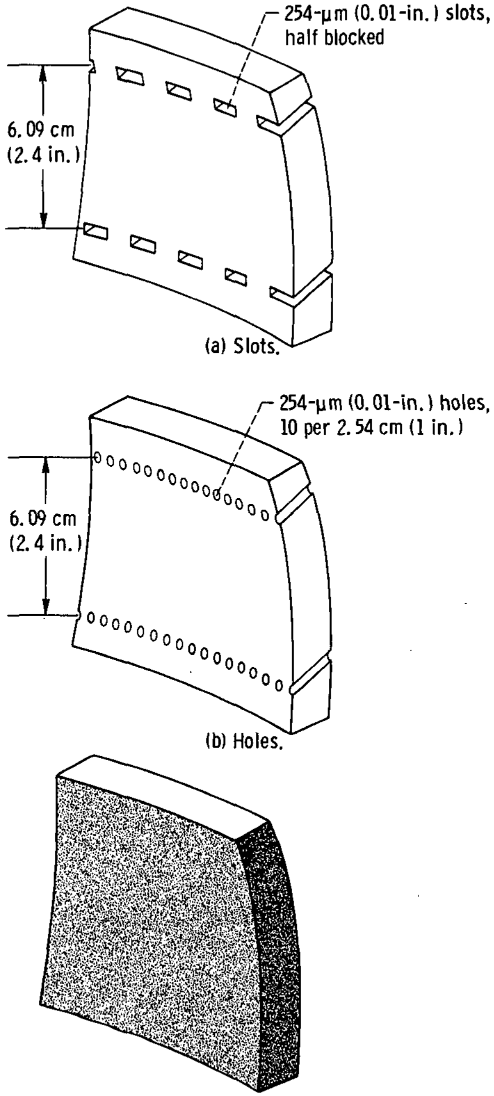


(a) Slots.

(b) Holes.

(c) Permeable media.

Figure 10. - Various propellant injection configurations.

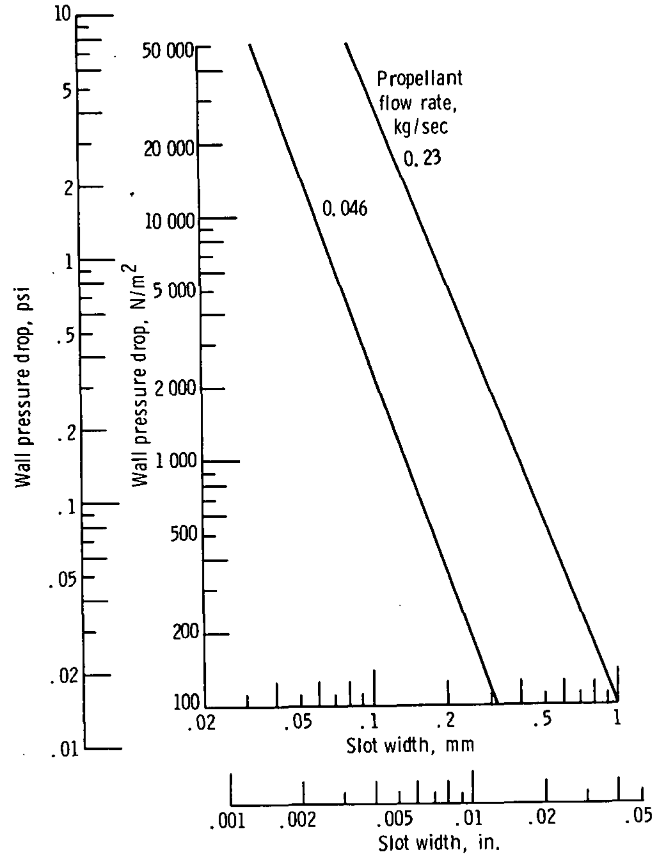


Figure 11. - Cavity wall pressure drop for various injection slot widths.

*"The aeronautical and space activities of the United States shall be conducted so as to contribute . . . to the expansion of human knowledge of phenomena in the atmosphere and space. The Administration shall provide for the widest practicable and appropriate dissemination of information concerning its activities and the results thereof."*

—NATIONAL AERONAUTICS AND SPACE ACT OF 1958

# NASA SCIENTIFIC AND TECHNICAL PUBLICATIONS

TECHNICAL REPORTS: Scientific and technical information considered important, complete, and a lasting contribution to existing knowledge.

TECHNICAL NOTES: Information less broad in scope but nevertheless of importance as a contribution to existing knowledge.

TECHNICAL MEMORANDUMS: Information receiving limited distribution because of preliminary data, security classification, or other reasons. Also includes conference proceedings with either limited or unlimited distribution.

CONTRACTOR REPORTS: Scientific and technical information generated under a NASA contract or grant and considered an important contribution to existing knowledge.

TECHNICAL TRANSLATIONS: Information published in a foreign language considered to merit NASA distribution in English.

SPECIAL PUBLICATIONS: Information derived from or of value to NASA activities. Publications include final reports of major projects, monographs, data compilations, handbooks, sourcebooks, and special bibliographies.

TECHNOLOGY UTILIZATION PUBLICATIONS: Information on technology used by NASA that may be of particular interest in commercial and other non-aerospace applications. Publications include Tech Briefs, Technology Utilization Reports and Technology Surveys.

*Details on the availability of these publications may be obtained from:*

SCIENTIFIC AND TECHNICAL INFORMATION OFFICE
NATIONAL AERONAUTICS AND SPACE ADMINISTRATION
Washington, D.C. 20546